2007-01-01

Aeronautical telemetry using multiple-antenna transmitters

Michael A. Jensen
jensen@byu.edu

Michael D. Rice
mdr@byu.edu

See next page for additional authors

Original Publication Citation
Jensen, M. A., M. D. Rice, and A. L. Anderson. "Aeronautical Telemetry using Multiple-Antenna Transmitters." Aerospace and Electronic Systems, IEEE Transactions on 43.1 (27): 262-72

Aeronautical Telemetry using Multiple-Antenna Transmitters

MICHAEL A. JENSEN, Senior Member, IEEE
MICHAEL D. RICE, Senior Member, IEEE
ADAM L. ANDERSON, Student Member, IEEE
Brigham Young University

The placement of multiple antennas on an air vehicle is one possible practice for overcoming signal obstruction created by vehicle maneuvering during air-to-ground transmission. Unfortunately, for vehicle attitudes where more than one of these antennas has a clear path to the receiving station, this practice also leads to self-interference nulls, resulting in dramatic degradation in the average signal integrity. This paper discusses application of unitary space-time codes such as the Alamouti transmit diversity scheme and unitary differential space-time codes to overcome the self-interference effect observed in such systems. The mathematical foundations of these techniques within the context of this application as well as computational performance gains associated with their implementation are provided. Issues such as the cost of channel estimation for trained techniques as well as the throughput performance of nondifferential and differential schemes for realistic air-vehicle motion are analyzed.

Manuscript received July 14, 2005; revised March 28, 2006; released for publication March 31, 2006.

IEEE Log No. T-AES/43/1/895633.

Refereeing of this contribution was handled by T. F. Roome.

Portions of this paper were presented at the International Telemetering Conference, San Diego, CA.

This work was supported by the U.S. Air Force under Contract F04611-02-C-0019, the National Science Foundation under Information Technology Research Grant CCR-0313056, and the U.S. Army Research Office under the Multi-University Research Initiative (MURI) Grant W911NF-04-1-0224.

Authors' address: Dept. of Electrical and Computer Engineering, 459 Clyde Bldg., Brigham Young University, Provo, UT 84602.

I. INTRODUCTION

The air-to-ground telemetry link is a key component of the test and evaluation of airborne systems such as aircraft and missiles. Historically, aircraft links were comprised of a transmit antenna mounted on the underside of the fuselage and a fixed ground station equipped with a tracking antenna as illustrated in Fig. 1(a). However, as depicted in Fig. 1(b), certain aircraft maneuvers can block the required line-of-sight propagation path. The traditional solution has been the use of two antennas radiating the same signal, with the typical placement of one antenna on the bottom and another on the top of the fuselage, to maintain the link for these maneuvers as shown in Fig. 1(c).

While this configuration is effective for overcoming data outages due to signal obstruction, difficulties arise when both antennas have a clear view to the ground station. In this case, the two signals arrive at the receiver with different angle-dependent phase shifts resulting in destructive interference for certain vehicle attitudes. The two-antenna system therefore behaves as a single array with an undesirable gain pattern, as illustrated in Fig. 1(d) [1–3]. When the antennas are separated both longitudinally and vertically on the fuselage, the antenna gain pattern variations are dramatic in azimuth and elevation angles, leading to signficant signal fluctuations for simple turns [4] as well as more aggressive maneuvers such as rolls and loops. The resulting signal outages during flight often require test flights to be performed multiple times, inserting costly delays in the system evaluation process.

Several solutions to this problem have been considered. One simple approach is to use different carrier frequencies for the two antennas, although this doubles the bandwidth requirement and can claim the use of two ground station antennas. The 1997 reallocation of 60 MHz in the lower S-band from aeronautical telemetry to commercial uses coupled with the increasing data rate requirements for modern tests have made it so that the test community cannot tolerate increased bandwidth requirements. Another solution to this problem is to equip the aircraft with a steerable antenna to ensure that the ground station is always in the array pattern main beam. However, this solution requires high resolution time-space position and aircraft attitude information as well as sophisticated on-board processing capability and antenna technology.

We view the system as a simple multiple-input multiple-output (MIMO) communication link with two transmit antennas and one receive antenna and show that space-time coding [5, 6] overcomes the limitations described above with no additional bandwidth requirement. This approach also permits a straightforward generalization to

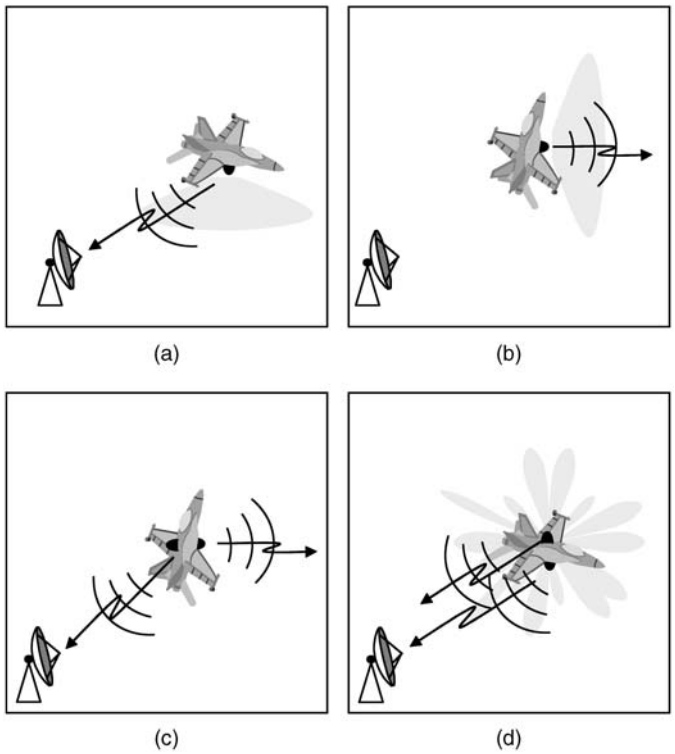

Fig. 1. Illustration of the basic problem of dual-antenna air-to-ground communication. (a) Air-to-ground link for normal, level flight. (b) Line-of-sight propagation from a single antenna can be blocked during maneuvers. (c) Use of two transmit antennas can solve this coverage problem. (d) When the same signal is transmitted from both antennas, self-interference results and has the same effect as a composite antenna with a very poor beam pattern.

include additional antennas at the transmitter and/or receiver. In determining which space-time codes to use, we require that the system 1) maintain full operation when the signal from one transmit antenna is fully obstructed, and 2) provide aircraft attitude-independent performance. We show that the popular class of unitary space-time block codes [7] satisfy these constraints and demonstrate the effectiveness of the Alamouti code [8] (which requires channel estimation using pilot symbols) and unitary differential codes [9, 10] (which do not require channel estimation, but are not full rate). We compare the performance of these codes in a time-varying channel created by a real aircraft maneuver using quadrature phase shift-keying (QPSK) symbols. Throughput and bit error rate (BER) degradations due to practical channel estimation are included in the comparison. The results indicate that, in this environment, the Alamouti code offers superior throughput but inferior BER relative to the differential codes (which offer a coding gain [9]).

II. SYSTEM MODEL

In this paper, boldface uppercase and lowercase letters are used to represent matrices and vectors, respectively, with h_m representing the mth element of the vector $\mathbf{h}$ and H_{mn} representing the element occupying the mth row and nth column of the matrix $\mathbf{H}$.

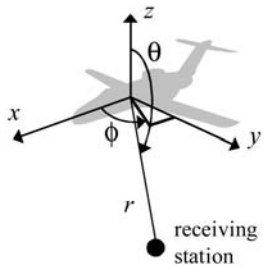

Fig. 2. Geometry of an airplane with two antennas communicating with a single receiver.

A. Antenna Representation

In the following, we assume that the mth transmit antenna is located at (x_m, y_m, z_m) expressed in a local coordinate frame for the air vehicle (see Fig. 2). The receiving station is located at the point (r, θ, ϕ) in spherical coordinates again in the vehicle coordinate frame. The complex field radiation pattern for the mth antenna (element pattern), which includes the effect of obstruction by the air vehicle, is $f_m(\theta, \phi)$. Using fundamental concepts from antenna theory [11], the electric field at the receiver due to unit excitation on the mth antenna may be expressed as

$$h_m(\theta,\phi) = f_m(\theta,\phi)\exp[jk(x_m\sin\theta\cos\phi + y_m\sin\theta\sin\phi + z_m\cos\theta)] \quad (1)$$

where $k = 2\pi/\lambda$ is the free-space wavenumber with λ the free-space wavelength. In the remainder of this paper, we refer to (1) as the transfer function for the mth antenna. Note that we have neglected the term e^{-jkr}/r and the pattern of the receive antenna as these are the same for all m. For time-varying distance r to the receiver, the e^{-jkr} term creates a Doppler shift which we assume is tracked by a frequency lock loop in the receiver.

B. Space-Time Block Code Representation

Assume a general system with M transmit antennas and a single receive antenna. The channel from the transmit elements to the receiver is denoted by the row vector $\mathbf{h}$ with elements $h_m(\theta,\phi)$, $1 \le m \le M$. A space-time block code transmits N symbols from the M transmit antennas during an interval corresponding to N symbol times. Arranging the symbols transmitted from each antenna into a space-time code matrix leads to the form

$$\mathbf{C}^{(n)} = \kappa \begin{bmatrix} c_1^{(n)} & c_1^{(n+1)} & \cdots & c_1^{(n+N-1)} \\ c_2^{(n)} & c_2^{(n+1)} & \cdots & c_2^{(n+N-1)} \\ \vdots & \vdots & \ddots & \vdots \\ c_M^{(n)} & c_M^{(n+1)} & \cdots & c_M^{(n+N-1)} \end{bmatrix} \quad (2)$$

where $c_m^{(n)}$ represents the symbol transmitted from the mth antenna during the nth symbol time and κ is a scaling constant. Assuming one sample per symbol from the receiver matched filter output, the complex baseband received signal is given by the row vector

$$\mathbf{r}^{(n)} = \mathbf{h}\mathbf{C}^{(n)} + \boldsymbol{\eta}^{(n)} \quad (3)$$

where $\boldsymbol{\eta}^{(n)}$ is an N-dimensional row vector with elements representing zero-mean additive white Gaussian noise (AWGN).

III. GOOD SPACE-TIME CODES

Our goal is to identify the properties of the code matrix $\mathbf{C}^{(n)}$ given by (2) that lead to reliable communication during aggressive air vehicle maneuvering. In so doing, we recognize that the code must maintain a strong link when the signal from one (or possibly more) of the antennas is obstructed. Furthermore, when multiple transmitted signals arrive at the receiver, the coding must be performed to remove any self-interference. We separately formulate the code properties required to achieve each of these two outcomes.

A. Transmit Diversity

In traditional transmit diversity for multipath communications, the goal is to increase the probability of a strong link when the signal from one of the transmit antennas is weak (due to the multipath interference) at the receiver. In the communication channel considered here, the same kind of multipath interference does not exist, but we do encounter signal attenuation due to obstruction of one or more antennas by the vehicle. Given this connection, we can use recent results relating to traditional transmit diversity to assist in the code design [12]. In order for the two-antenna transmit system to provide full performance when one (or more, in the case of more than two transmit antennas) of the transmit antennas is blocked, the space-time code must exhibit full diversity. The diversity performance of the space-time code is dominated by the differences between matrices in the set of all possible code matrices. Specifically, let $\mathbf{C}_\alpha$ and $\mathbf{C}_\beta$ be two different possible code matrices. The singular value decomposition (SVD) of their difference is

$$\mathbf{C}_\beta - \mathbf{C}_\alpha = \mathbf{U}\boldsymbol{\Sigma}\mathbf{V}^\dagger \quad (4)$$

where $\mathbf{U}$ and $\mathbf{V}$ are $M \times M$ and $N \times N$ unitary matrices, respectively, $\boldsymbol{\Sigma}$ is $M \times N$ with elements $\sigma_{mn} = 0$ for $m \ne n$, and $\{\cdot\}^\dagger$ indicates a conjugate transpose. It has been shown that full diversity can be achieved for $N \ge M$ [12]. Since $N = M$ uses the minimum number of symbol times to create this diversity, analysis based on the assumption $N = M$ produces a lower bound on the diversity performance. Under this condition the code matrices are square and, for maximum likelihood (ML) detection, the ideal code matrices for diversity performance satisfy the criterion [12]

$$\boldsymbol{\Sigma}\boldsymbol{\Sigma}^\dagger = a\mathbf{I} \quad (5)$$

where a is a constant. This relationship must hold for each possible pair of code matrices.

B. Angular Power Distribution

When the signals from multiple (unobstructed) antennas arrive at the receiver, they will mutually interfere, resulting in transmission nulls for certain air-vehicle attitudes if the code is improperly designed. If the transmitter tracks the direction to the receiver, beamforming techniques can be used to maximize the received power. However, in the practical scenario where direction tracking is infeasible, we must design the code such that the radiated power averaged over the time interval of the code matrix is uniform in angle, as this will ensure uniform performance regardless of the vehicle attitude.

The key to solving this problem lies in recognizing that the complex weighting created by each column of the code matrix $\mathbf{C}^{(n)}$ creates a distinct radiation pattern for each symbol time. Let the electric field

radiation pattern of the transmit array during the nth symbol time be represented as $q^{(n)}(\theta,\phi)$. The row vector of the N radiation patterns created during the code transmission becomes

$$\mathbf{q}^{(n)}(\theta,\phi) = \mathbf{h}\mathbf{C}^{(n)} \tag{6}$$

and the radiated power distribution time-averaged over this code duration is

$$\frac{1}{N}\sum_{n=1}^{N}|q^{(n)}(\theta,\phi)|^2 = \frac{1}{N}\mathbf{q}^{(n)}\mathbf{q}^{(n)\dagger} = \frac{1}{N}\mathbf{h}\mathbf{C}^{(n)}\mathbf{C}^{(n)\dagger}\mathbf{h}^{(n)\dagger}. \tag{7}$$

We assume $f_m(\theta,\phi) = 1$, since the code can only realistically control the array pattern and not compensate for variations in the element patterns. In this case, the terms $h_m(\theta,\phi)h_m^*(\theta,\phi) = 1$ are independent of angle while the terms $h_m(\theta,\phi)h_{m'}^*(\theta,\phi)$ are angle dependent for $m' \neq m$. The only way to remove the effect of these angle-dependent terms for all angles (θ,ϕ) is to require $\mathbf{C}^{(n)}\mathbf{C}^{(n)\dagger}$ to be diagonal. Also, to be consistent with the discussion in Section IIIA, if masking occurs then the code performance should not depend on which element(s) is masked. Therefore, all the diagonal elements in $\mathbf{C}^{(n)}\mathbf{C}^{(n)\dagger}$ should be the same; that is

$$\mathbf{C}^{(n)}\mathbf{C}^{(n)\dagger} = b\mathbf{I} \tag{8}$$

with b a constant. In other words, the code must be (scaled) unitary.

IV. SPECIFIC SIGNALING APPROACHES

We now consider several specific signaling strategies for transmission from a maneuvering air vehicle for two antennas ($M = N = 2$). Our analysis includes transmitting from a single antenna and transmitting the same symbol from each of two antennas to illustrate the poor performance obtained when proper signaling is not applied. As examples of appropriate codes, we discuss Alamouti and unitary differential space-time codes for dual-antenna transmission. In all of the following, we assume a sequential set of symbols $s^{(n)}, s^{(n+1)}, \ldots, s^{(n+N-1)}$ are to be transmitted, with the average symbol energy represented as E_s. Also, the complex noise waveform has real and imaginary parts each with power spectral density $N_0/2$, so that for complex signaling the variance of the noise samples $\eta_m^{(n)}$ is the same for all antennas and has a value of $\sigma_\eta^2 = N_0$ [13].

For all cases considered here except for the differential codes, a closed-form expression for the BER is possible. We demonstrate this analysis assuming that the symbols $s^{(n)}$ are drawn from the QPSK constellation such that the bit energy $E_b = E_s/2$, although the procedure easily generalizes to other linear modulations. If $p_{\theta\phi}(\theta,\phi)$ is the probability density function (pdf) of the angles to the receiver encountered during the maneuver, then the average BER for the maneuver is [13]

$$P(e) = \int_0^{2\pi}\int_0^{\pi} Q\left(\sqrt{\frac{2E_b}{N_0}\alpha(\theta,\phi)}\right) p_{\theta\phi}(\theta,\phi)\sin\theta\, d\theta\, d\phi \tag{9}$$

where

$$Q(x) = \frac{1}{\sqrt{2\pi}}\int_x^{\infty} e^{-t^2/2}dt.$$

The scale-factor $\alpha(\theta,\phi)$ is derived in the following sections for the different signaling schemes under consideration. The pdf $p_{\theta\phi}(\theta,\phi)$ can either be estimated based on knowledge of a maneuver/typical flight profile or numerically constructed from a flight simulation.

A. Single Antenna Transmission

Consider first transmission using only one antenna ($m = 1$). The code matrix has the form

$$\mathbf{C}_s^{(n)} = \begin{bmatrix} s^{(n)} & s^{(n+1)} \\ 0 & 0 \end{bmatrix}. \tag{10}$$

Since only one symbol is transmitted, the expression in (9) is applicable. It is straightforward to show that

$$\alpha(\theta,\phi) = |h_1(\theta,\phi)|^2 \tag{11}$$

where $h_1(\theta,\phi)$ is related to the antenna radiation pattern and aircraft attitude by (1). It is easy to verify that the 16 possible code matrices $\mathbf{C}_s^{(n)}$ do not satisfy the full diversity condition (5) nor the angle-independent condition (8).

B. Uncoded Dual-Antenna Transmission

For uncoded two-antenna transmission, each symbol is simultaneously radiated from both antennas. The code matrix for this case has the form

$$\mathbf{C}_u^{(n)} = \frac{1}{\sqrt{2}}\begin{bmatrix} s^{(n)} & s^{(n+1)} \\ s^{(n)} & s^{(n+1)} \end{bmatrix} \tag{12}$$

where the factor of $\sqrt{2}$ comes from the equal division of the power between the two antennas. Once again only one symbol is transmitted per symbol time so that (9) applies with

$$\alpha(\theta,\phi) = \tfrac{1}{2}|h_1(\theta,\phi) + h_2(\theta,\phi)|^2. \tag{13}$$

It is again easy to show that the 16 possible code matrices $\mathbf{C}_u^{(n)}$ satisfy neither the full diversity condition (5) nor the angle-independent condition (8).

The term $|h_1(\theta,\phi) + h_2(\theta,\phi)|^2$ effectively represents the radiation pattern of the two-element array. For widely-spaced antennas[1] and narrowband signaling,

[1]Widely spaced antennas are typical of the situation for dual-antenna aeronautical systems where the goal is to provide communication reliability against signal obstruction.

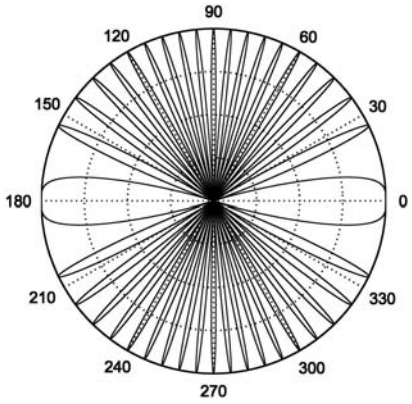

Fig. 3. Gain pattern versus ϕ resulting from 2 antennas separated by 10λ for $\theta = 90°$.

this array radiation pattern will be characterized by a large number of nulls. For example, Fig. 3 illustrates a plot of $|h_1(\theta,\phi) + h_2(\theta,\phi)|^2$ as a function of the angle ϕ for $\theta = 90°$ with the antennas separated by 10λ in the x dimension and assuming $f_m(\theta,\phi) = 1$. This highly variable behavior in the received signal strength and therefore signal-to-noise ratio (SNR) is the source of the link outages observed at test ranges. With wideband signaling where the radiation pattern nulls are frequency dependent, the effective loss in received power will be somewhat mitigated.

C. Alamouti Dual-Antenna Transmission

For the Alamouti transmit diversity scheme [8], the code matrix is given by

$$\mathbf{C}_a^{(n)} = \frac{1}{\sqrt{2}} \begin{bmatrix} s^{(n)} & -s^{(n+1)*} \\ s^{(n+1)} & s^{(n)*} \end{bmatrix}. \tag{14}$$

It is easy to show that this matrix is (scaled) unitary so that it satisfies the angle-independent condition (8) and that the 16 possible matrices $\mathbf{C}_a^{(n)}$ satisfy (5). Furthermore, we can modify the expression for the received signal as

$$\begin{aligned} \mathbf{r}_a^{(n)} &= [r^{(n)} \quad r^{(n+1)*}] \\ &= \frac{1}{\sqrt{2}} \mathbf{s}^{(n)} \underbrace{\begin{bmatrix} h_1(\theta,\phi) & h_2^*(\theta,\phi) \\ h_2(\theta,\phi) & -h_1^*(\theta,\phi) \end{bmatrix}}_{\mathbf{H}} + \boldsymbol{\eta}_a^{(n)} \end{aligned} \tag{15}$$

where $\mathbf{s}^{(n)} = [s^{(n)} \;\; s^{(n+1)}]$ and $\boldsymbol{\eta}_a^{(n)} = [\eta^{(n)} \;\; \eta^{(n+1)*}]$. It is then straightforward to show that symbol detection can be performed using the operation

$$\begin{aligned} \hat{\mathbf{r}}_a^{(n)} &= \mathbf{r}_a^{(n)} \mathbf{H}^\dagger \\ &= \frac{1}{\sqrt{2}} (|h_1(\theta,\phi)|^2 + |h_2(\theta,\phi)|^2) \mathbf{s}^{(n)} + \boldsymbol{\eta}_a^{(n)} \mathbf{H}^\dagger. \end{aligned} \tag{16}$$

Since this operation has decoupled the two symbols in time, (9) applies with

$$\alpha(\theta,\phi) = \tfrac{1}{2}(|h_1(\theta,\phi)|^2 + |h_2(\theta,\phi)|^2). \tag{17}$$

This result emphasizes the angle-independent average power distribution for isotropic element patterns ($f_m = 1$) since $|h_m(\theta,\phi)| = 1$ under this condition.

Equation (16) reveals that implementing the Alamouti scheme requires that the receiver determine the transfer functions $h_1(\theta,\phi)$ and $h_2(\theta,\phi)$. Furthermore, the closed-form BER expression assumes this channel state information (CSI) is known perfectly at the receiver. In practical implementation, CSI would likely be obtained via periodic transmission of training sequences, introducing errors in the CSI due to imperfect estimation. The change in the channel between training cycles introduces further error. These errors lead to an increase in the BER, and the transmission of known training symbols reduces the useful system throughput.

Computational results shown later include the effects of CSI estimation errors when appropriate. This estimation is performed by transmitting a known sequence of N_T symbols. Assuming that the channel remains approximately constant during this training interval, the received sequence of matched filter outputs can be expressed as

$$\mathbf{r}_T^{(n)} = \mathbf{h}\mathbf{S}_T^{(n)} + \boldsymbol{\eta}_T^{(n)} \tag{18}$$

where each 2×2 block of the $2 \times N_T$ matrix $\mathbf{S}_T^{(n)}$ is an Alamouti code matrix containing training symbols. The maximum likelihood (ML) estimate of the channel transfer functions assuming zero-mean independent Gaussian noise is then given as [14]

$$\hat{\mathbf{h}} = \mathbf{r}_T^{(n)} \mathbf{S}_T^{(n)+} \tag{19}$$

where $\{\cdot\}^+$ represents a matrix pseudoinverse. To avoid an underdetermined linear system, $N_T \geq 2$, with larger values of N_T generally resulting in improved channel estimates. Using this estimator, the mean and covariance of the channel estimates $\hat{\mathbf{h}}$ are

$$\mathrm{E}\{\hat{\mathbf{h}}\} = \mathbf{h} \tag{20}$$

$$\mathrm{E}\{(\hat{\mathbf{h}} - \mathbf{h})^\dagger (\hat{\mathbf{h}} - \mathbf{h})\} = \frac{2\sigma_\eta^2}{N_T E_s} \mathbf{I}. \tag{21}$$

Thus, the estimator is unbiased and efficient (since the covariance meets the Cramér-Rao bound [15]). Note that the variance of the estimate decreases as the number of pilot symbols N_T increases. However, the effective throughput of the system decreases as N_T increases. Thus, the number of pilot symbols should be chosen to balance the effect of channel estimation errors with throughput reduction. This trade-off is explored in Section V.

D. Differential Transmission

One alternative approach to implementation of the Alamouti transmission scheme is to use a differential

space-time modulation [9, 10] that does not require estimation of CSI at the receiver. Because we have focused our attention on QPSK symbols, we here consider the quaternion code [9] constructed from these symbols and consisting of the eight constellation matrices ($\mathcal{G}$) and the initialization matrix (**D**) [9]

$$\mathcal{G} = \left\{ \pm \begin{bmatrix} 1 & 0 \\ 0 & 1 \end{bmatrix}, \pm \begin{bmatrix} j & 0 \\ 0 & -j \end{bmatrix} \pm \begin{bmatrix} 0 & 1 \\ -1 & 0 \end{bmatrix}, \pm \begin{bmatrix} 0 & j \\ j & 0 \end{bmatrix} \right\} \tag{22}$$

$$\mathbf{D} = \frac{1}{\sqrt{2}} \begin{bmatrix} 1 & -1 \\ 1 & 1 \end{bmatrix}. \tag{23}$$

Transmission begins by sending $\mathbf{C}^{(0)} = \mathbf{D}$ during the first block interval. Each additional transmission is then encoded as $\mathbf{C}^{(n)} = \mathbf{C}^{(n-1)}\mathbf{G}^{(n)}$, where $\mathbf{G}^{(n)}$ represents one of the matrices from the constellation $\mathcal{G}$. After transmission of this code matrix through the channel, the ML differential detector for estimating the transmitted matrix is given as [9]

$$\hat{\mathbf{G}}^{(n)} = \arg\max_{\mathcal{G}} \operatorname{Re} \operatorname{Tr}\{\mathbf{G}\mathbf{r}^{(n)\dagger}\mathbf{r}^{(n-1)}\} \tag{24}$$

where Re Tr$\{\cdot\}$ means the real part of the matrix trace. Unlike in the case of Alamouti signaling, the channel transfer vector is not required in the detection implementation. We also point out that the performance of this detector cannot be evaluated using the closed-form BER expression in (9).

The quaternion code offers the same diversity performance and, since the code blocks are scaled unitary matrices, angle-independent power radiation provided by the Alamouti code. However, since there are eight possible points in the constellation $\mathcal{G}$, each matrix block represents transmission of three bits in contrast to the four bits per code matrix offered by the Alamouti code with QPSK symbols. Therefore, differential modulation results in a reduced rate (and in exchange offers increased coding gain) relative to the Alamouti code [9].

V. COMPUTATIONAL RESULTS

The evaluation of the transmission strategies discussed in Section IV are performed using a combination of the closed-form BER expression in (9) and detailed simulations that compute the transfer functions $h_m(\theta, \phi)$ for realistic flight maneuvers. For the latter case, the air vehicle motion is characterized by an initial position, velocity, attitude (yaw, pitch, and roll), and a rotation rate for each of the attitude angles. Using Eulerian angle transformations [16, 17], the angular position of the ground station in the vehicle coordinate frame is computed at each sample time (one sample per transmitted symbol). This angle information is then used to compute $h_m(\theta, \phi)$ as in (1).

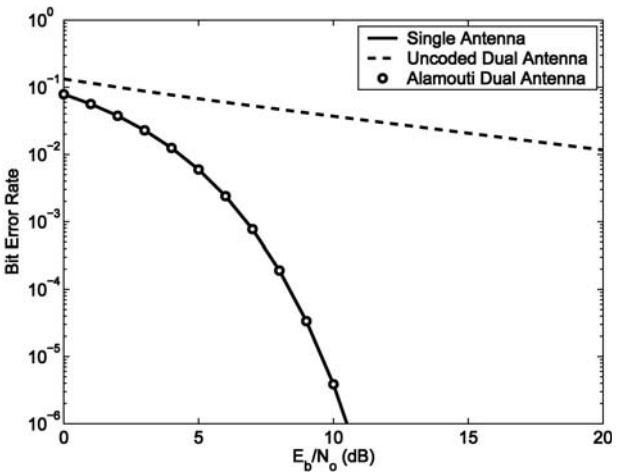

Fig. 4. BER versus E_b/N_0 for an air vehicle engaged in a roll for single antenna, uncoded dual antenna, and Alamouti dual antenna transmission with QPSK symbols evaluated using the closed-form BER solution. Antenna obstruction is neglected.

In all of the following computations, we assume that antennas 1 and 2 are placed at $(0,0,0)$ and $(10,0,10)$, respectively, where the dimensions are in wavelengths (10 wavelengths = 2 m at 1.5 GHz). Unless explicitly stated, the element radiation patterns are isotropic ($f_m = 1$). Flight simulations assume that the air vehicle travels at 300 m/s and is initially 3000 m away from the ground station (horizontally) at an altitude of 2000 m above ground. The initial direction of flight is perpendicular to the line between the aircraft and ground station, and the vehicle is engaged in a roll at 1 rev/s. The QPSK communication is performed at 1 Msymbol/s, and 5×10^6 symbols are sent to determine the BER performance.

A. Analytic BER Computation

As a first example, we assess the performance during a simple air vehicle roll with $p_{\theta\phi}(\theta, \phi) = \delta(\phi - \pi/2)/2\pi$ using the closed-form BER analysis of (9). These results are plotted versus E_b/N_0 in Fig. 4 for single antenna, uncoded dual antenna, and Alamouti dual antenna transmission schemes. The impact of self-interference for uncoded dual antenna transmission is dramatic, while the Alamouti scheme completely eliminates this interference as predicted.

To model the effect of antenna obstruction, the element radiation patterns are modified to be

$$\begin{aligned} f_1(\theta, \phi) &= \begin{cases} 0 & 0 \le \theta < \theta_o \\ 1 & \text{otherwise} \end{cases} \\ f_2(\theta, \phi) &= \begin{cases} 0 & \pi - \theta_o \le \theta < \pi \\ 1 & \text{otherwise} \end{cases} \end{aligned} \tag{25}$$

where θ_o specifies the angular extent of the masking and is chosen to simulate obstruction of each antenna for a specified percentage of the time during the

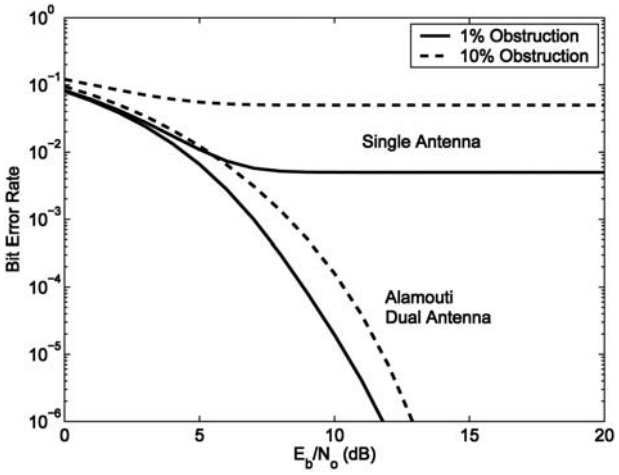

Fig. 5. BER versus E_b/N_0 for an air vehicle engaged in a roll for single antenna and Alamouti dual antenna transmission with QPSK symbols evaluated using the closed-form BER solution. Signal from each antenna is obstructed 1% or 10% of the time during the maneuver.

maneuver. This parametric form is not physically realistic due to the abrupt nature of the obstruction, but facilitates an intuitive understanding of the BER performance versus masking extent. Fig. 5 plots the BER performance for single antenna and Alamouti transmission for the roll maneuver assuming obstruction occurs 1% ($\theta_o = \pi/100$) and 10% ($\theta_o = \pi/10$) of the time. As can be seen, the single antenna performance is dramatically reduced, reaching a high-SNR bound determined by the masking behavior (0.5 BER during masking multiplied by the percentage of time masked). In contrast, the spatial diversity offered by the Alamouti scheme makes it robust to obstruction of one signal, with the performance reduction due only to the decrease in average received power during masking. This analysis also allows us to anticipate the impact of a different angular pdf $p_{\theta\phi}(\theta,\phi)$ on the performance. For example, a manuever with an increased probability of masking one of the antennas will result in a higher BER floor for single antenna transmission and shift the curve to the right for Alamouti transmission.

B. Effects of Channel Estimation

Two key effects must be examined when considering errors due to imperfect CSI at the receiver. The first involves the accuracy of the channel estimate constructed from noisy received training data. While fully characterizing the impact of this error for the ML estimator of (19) requires detailed simulations for a given flight maneuver, significant insight can be obtained from a closed-form analysis approach. Specifically, let the estimated channel vector be represented as

$$\hat{\mathbf{h}} = \mathbf{h} + \boldsymbol{\delta} \tag{26}$$

where $\boldsymbol{\delta} = [\delta_1(\theta,\phi), \delta_2(\theta,\phi)]$ represents the channel estimate error vector whose elements are independent zero-mean Gaussian random variables with variance given by (21). To use this covariance in estimating the BER versus training sequence length and SNR, we rewrite (16) as

$$\begin{aligned}\hat{\mathbf{r}}_a^{(n)} &= \frac{1}{\sqrt{2}}\mathbf{s}^{(n)}\mathbf{H}(\mathbf{H}+\boldsymbol{\Delta})^\dagger + \boldsymbol{\eta}_a^{(n)}(\mathbf{H}+\boldsymbol{\Delta})^\dagger \\ &\approx \underbrace{\frac{1}{\sqrt{2}}\mathbf{s}^{(n)}[(|h_1|^2+|h_2|^2)\mathbf{I} + (\mathbf{H}\boldsymbol{\Delta}^\dagger)_d]}_{\mathbf{H}_e} \\ &\quad + \underbrace{\left[\frac{1}{\sqrt{2}}\mathbf{s}^{(n)}(\mathbf{H}\boldsymbol{\Delta}^\dagger)_o + \boldsymbol{\eta}_a^{(n)}\mathbf{H}^\dagger\right]}_{\boldsymbol{\eta}_e^{(n)}},\end{aligned} \tag{27}$$

where $\boldsymbol{\Delta}$ is the channel coefficient errors arranged in the Alamouti channel matrix form (see (15)) and we have dropped the functional dependence in $h_m(\theta,\phi)$ for simplicity. We have isolated the diagonal terms $(\mathbf{H}\boldsymbol{\Delta}^\dagger)_d$ and off-diagonal terms $(\mathbf{H}\boldsymbol{\Delta}^\dagger)_o$ such that $\mathbf{H}_e$ is diagonal and the remainder of the expression can be considered effective noise $\boldsymbol{\eta}_e^{(n)}$. Also, we have neglected the term $\boldsymbol{\eta}_a^{(n)}\Delta^\dagger$ which is small for high SNR.

Taking each element of the vector in (27) individually, the expression is of the same form as that considered in communication over Ricean fading channels by Lindsey [18]. The probability of bit error is given by

$$\begin{aligned}P_b &= Q(u,w) - \frac{1}{2}\left[1+\sqrt{\frac{d}{1+d}}\right] \\ &\quad \times \exp\left\{-\frac{u^2+w^2}{2}\right\} \mathrm{I}_0(uw)\end{aligned} \tag{28}$$

where

$$u = \sqrt{\frac{|h_1|^2+|h_2|^2}{\sigma_\Delta^2} \times \frac{1+2d-2\sqrt{d(1+d)}}{2(1+d)}} \tag{29}$$

$$w = \sqrt{\frac{|h_1|^2+|h_2|^2}{\sigma_\Delta^2} \times \frac{1+2d+2\sqrt{d(1+d)}}{2(1+d)}} \tag{30}$$

$$d = \frac{1}{2(1+N_T)} \tag{31}$$

$$\sigma_\Delta^2 = \frac{2\sigma_\eta^2}{N_T E_s} \tag{32}$$

and $\mathrm{I}_0(x)$ is zero-th order modified Bessel function.

The top plot in Fig. 6 shows the BER versus E_b/N_0 obtained using this formulation for $N_T = 8$ training symbols compared with that obtained from 5×10^6 Monte Carlo simulations where the channel estimation is performed directly with the ML estimator of (19). As can be seen, the closed-form analysis accurately predicts the system performance.

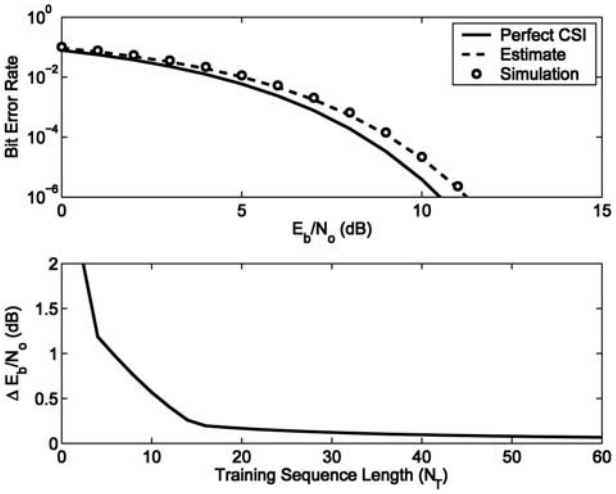

Fig. 6. Top Plot: BER versus E_b/N_0 for a training sequence of length $N_T = 8$ obtained from the approximate statistical analysis ("Estimate") and detailed system simulations. Result for perfect CSI is shown for comparison. Bottom Plot: Required increase in signal strength $\Delta E_b/N_0$ to achieve a BER of 10^{-5} relative to the case where perfect CSI is available as a function of N_T.

These results also demonstrate that, as expected, errors in the channel estimates imply that the value of E_b/N_0 required to achieve a target BER increases. The bottom plot in Fig. 6 shows this increase $\Delta E_b/N_0$ relative to the case where perfect CSI is available for a target BER of 10^{-5}. These results demonstrate that the required signal strength is relatively insensitive to training sequence length for $N_T \geq 16$.

The second issue related to channel estimation is the frequency with which the channel estimate must be updated. Some insight regarding this frequency can be obtained by examining how quickly the channel changes with vehicle motion, and how the Alamouti detection performance degrades as the channel coefficients depart from the assumed estimates. To accomplish this study, the aircraft is held at its initial position (velocity is zero) and engaged in a complete revolution in roll angle. The abrupt masking model of (25) is replaced with the spatially differentiable and therefore more physically realistic form

$$f_1(\theta,\phi) = \begin{cases} \sin\theta & \theta < \pi/2 \\ 1 & \theta \geq \pi/2 \end{cases}$$
$$f_2(\theta,\phi) = \begin{cases} 1 & \theta \leq \pi/2 \\ \sin\theta & \theta > \pi/2 \end{cases}. \quad (33)$$

We emphasize here that both (25) and (33) represent relatively simple example radiation patterns which allow evaluation of the algorithm operation. To use the analysis approach defined here to obtain accurate performance for realistic antennas on a vehicle, more detailed radiation patterns would need to be used, presumably based on measurements or simulations of the entire vehicle/antenna combination.

Only antenna 1, placed at $(0,0,10)$ wavelengths in the aircraft coordinate frame, is used in this study.

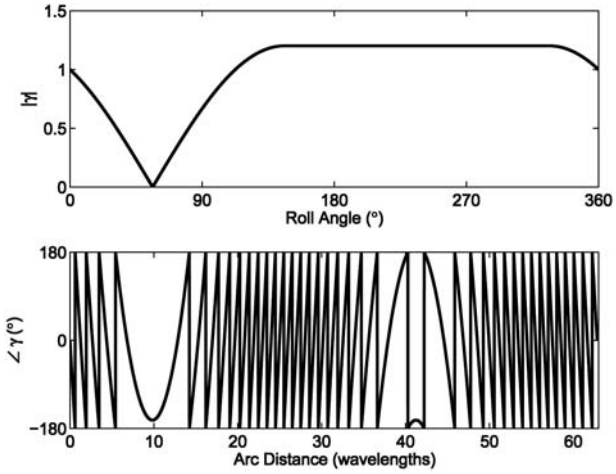

Fig. 7. Magnitude and phase of $\gamma = h_1(\theta,\phi)/\bar{h}$ during a roll maneuver ($\bar{h}$ is the channel transfer function at the initial point).

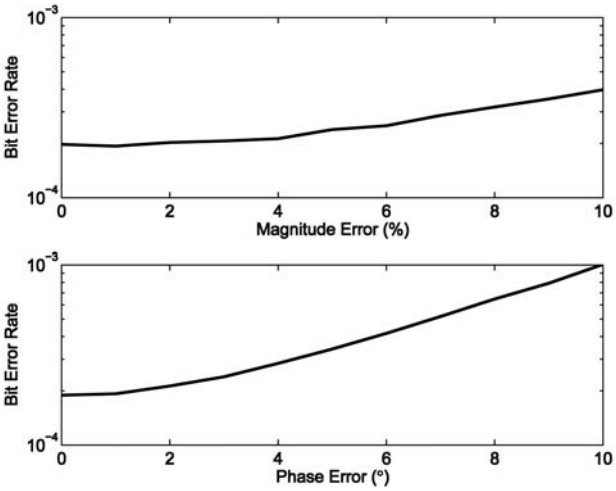

Fig. 8. BER versus channel estimate magnitude and phase error level for E_b/N_0=8 dB.

The value of the channel transfer function to this antenna at the initial position is represented as $\bar{h}$, and the quantity $\gamma(\theta,\phi) = h_1(\theta,\phi)/\bar{h}$ is constructed for the roll. Fig. 7 shows the magnitude and phase of γ for this maneuver. The magnitude is represented versus absolute roll angle, as this depends on the basic element radiation pattern. In contrast, the phase is plotted versus arc distance traveled (in wavelengths) of the antenna, since this distance will dominate the phase change for the transfer functions in (1). As can be seen, considerable change in the transfer function, particularly the phase, results from the motion. Fig. 8 reveals the impact of using a channel estimate whose magnitude and phase are in error on the BER performance of the Alamouti detection scheme (for $E_b/N_0 = 8$ dB). These results show that small magnitude errors cause a relatively small degradation in the BER. In contrast, phase errors of a few degrees can lead to noticeable impact on BER. In an operational system, therefore, the channel

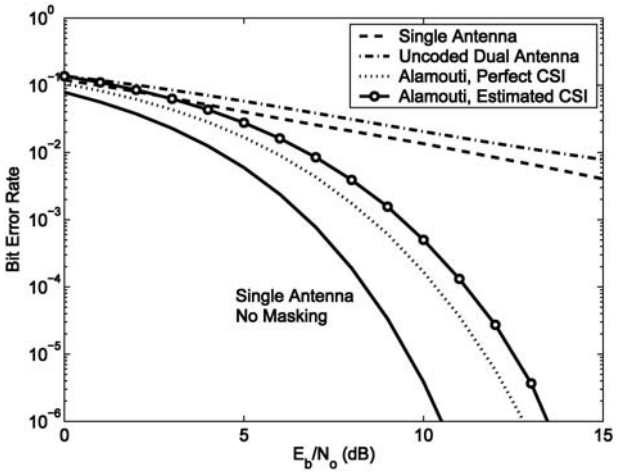

Fig. 9. BER versus E_b/N_0 obtained from a full system simulation for an aircraft engaged in a roll when channel estimation ($N_T = 8$, 5% of symbols devoted to training) and masking are included for various signaling schemes.

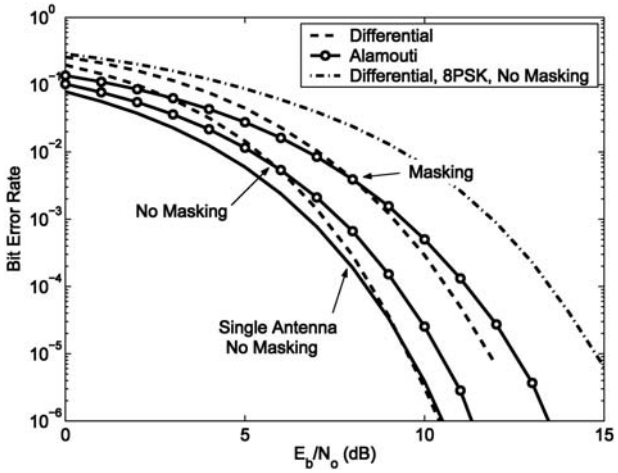

Fig. 10. Comparison of BER versus E_b/N_0 for differential and Alamouti codes using the full system simulation used for Fig. 9 with and without masking included. Results for differential codes using 8PSK symbols (no masking included) are also shown.

estimation should be performed after the phase has changed by a few degrees if possible. It is important to again emphasize that the phase change referred to is that created by the changing orientation of the vehicle relative to the receiving station and not the bulk phase (Doppler shift) created by the e^{-jkr} term common to both transmit antennas.

C. Full System Simulation

Fig. 9 shows the BER performance versus E_b/N_0 when the effect of signal obstruction (using (33)), vehicle motion, and channel estimation are included using a full system simulation. Channel estimation for this simulation uses training sequences with $N_T = 8$ symbols and 5% of the total number of symbols are devoted to training, parameters which appear to offer good BER performance. The single antenna results for this case differ from those in Fig. 5 due to the change in the masking model assumed. Despite this change, the results again illustrate the dramatic performance degradation for the single antenna transmission and modest performance impact for the Alamouti scheme when these realistic conditions are included.

D. Differential Code

Fig. 10 shows the performance of the differential code for simulations without and with antenna obstruction included (using (33)). Also shown for comparison are the results for Alamouti coding, where the training sequences of $N_T = 8$ symbols represent 5% of the total symbols transmitted. These results show that from the perspective of BER, the differential approach outperforms the Alamouti scheme as the SNR grows large, even if perfect channel estimates are available at the receiver, due to the higher coding gain of the differential code.

TABLE I
Transmission Rate and Increased Signal Strength (relative to single antenna transmission) Required to Achieve 10^{-5} BER for Different Transmission Schemes

Transmission Scheme		Rate	$\Delta E_b/N_0$ (dB)
Alamouti	$N_T = 8$	0.95	0.89
	$N_T = 16$	0.90	0.33
Differential	QPSK	0.75	0.00
	8PSK	1.00	5.10

It is important to keep in mind that the main drawback of the quaternion differential code is that it provides 3 bits per matrix block as compared with the 4 bits per block associated with Alamouti transmission using QPSK symbols. Therefore, provided that the channel variation is slow enough so that the fraction of bits devoted to training is less than 25%, the Alamouti scheme will provide increased throughput. To overcome this drawback, a differential code similar in form to the quaternion code that uses 8PSK symbols and provides 4 bits per block transmission can be constructed [9]. Fig. 10 also includes the BER curve for this case with no masking included. As can be seen, increasing the rate of the differential modulation produces a significant increase in the BER (or required SNR) due to the increased density of the underlying modulation constellation.

The relative performance of the Alamouti and differential codes are summarized in Table I which shows the effective transmission rate and required additional signal strength $\Delta E_b/N_0$ required to achieve 10^{-5} BER relative to a channel with a single, unmasked antenna for different signaling/training combinations. For the Alamouti code, the total number of training and data symbols for each block is held constant at 160, so that the training consumes 5% and 10% of the symbols for $N_T = 8$ and 16, respectively.

This drop accounts for the rate reduction below unity experienced for these two cases. The results in this table demonstrate the tradeoff between rate and signal power associated with the different signaling schemes considered.

VI. CONCLUSIONS

This paper has discussed the use of unitary space-time codes for providing robust communication between maneuvering air vehicles and a receiver. Specifically, design criteria for codes operating in this environment have been developed, and the performance of Alamouti and differential codes that satisfy these criteria has been evaluated for dual-antenna telemetry links. The analysis shows that in principle, these codes offer roughly the same performance as a single antenna while maintaining communication even when one antenna is masked by the air vehicle. Detailed analysis and simulations provide insight into the effect of channel estimation errors and the required frequency of training data transmission for the Alamouti code and demonstrate the behavior of both codes in realistic channels. The results suggest that these schemes are excellent candidates for implementation in practical air-vehicle communication systems.

REFERENCES

[1] Rice, M., and Law, G.
Aeronautical telemetry fading sources at test ranges.
In *Proceedings of the International Telemetering Conference*, Las Vegas, NV, Oct. 1997, 660–666.

[2] Pedroza, M.
Antenna pattern evaluation for link analysis.
In *Proceedings of the International Telemetering Conference*, San Diego, CA, Oct. 1996, 158–166.

[3] Reddemann, J.
Edwards range telemetry evaluation.
In *Proceedings of the International Test and Evaluation Association Conference*, Lancaster, CA, Apr. 1997.

[4] Jefferis, R.
Private communication.
Tybrin Corp., Edwards AFB, CA, 2000.

[5] Foschini, G. J., and Gans, M. J.
On limits of wireless communications in a fading environment when using multiple antennas.
Wireless Personal Communication, **6** (Mar. 1998), 311–335.

[6] Raleigh, G. G., and Cioffi, J. M.
Spatio-temporal coding for wireless communication.
IEEE Transactions on Communication, **46** (Mar. 1998), 357–366.

[7] Hochwald, B. M., Marzetta, T. L., Richardson, T. J., Sweldens, W., and Urbanke, R.
Systematic design of unitary space-time constellations.
IEEE Transactions on Information Theory, **46** (Sept. 2000), 1962–1973.

[8] Alamouti, S. M.
A simple transmit diversity technique for wireless communications.
IEEE Journal on Selected Areas of Communication, **16** (Oct. 1998), 1451–1458.

[9] Hughes, B.
Differential space-time modulation.
IEEE Transactions on Information Theory, **46** (Nov. 2000), 2567–2578.

[10] Hochwald, B. M., and Sweldens, W.
Differential unitary space-time modulation.
IEEE Transactions on Communication, **48** (Dec. 2000), 2041–2052.

[11] Balanis, C. A.
Antenna Theory: Analysis and Design.
New York: Wiley, 1997.

[12] Guey, J.-C., Fitz, M. P., Bell, M. R., and Kuo, W.-Y.
Signal design for transmitter diversity wireless communication systems over Rayleigh fading channels.
IEEE Transactions on Communication, **47** (Apr. 1999), 527–537.

[13] Proakis, J. G.
Digital Communications.
Mew York: McGraw-Hill, 1995.

[14] Scharf, L. L.
Statistical Signal Processing: Detection, Estimation, and Time Series Analysis.
Reading, MA: Addison-Wesley, 1991.

[15] Moon, T. K., and Stirling, W. C.
Mathematical Methods and Algorithms for Signal Processing.
Englewood Cliffs, NJ: Prentice-Hall, 2000.

[16] Rahmat-Samii, Y.
Useful coordinate transformations for antenna applications.
IEEE Transactions on Antennas Propagation, **AP-27** (July 1979), 571–574.

[17] Nielson, G. M
Smooth interpolation of orientations.
In D. Thalmann and N. Magnenat Thalmann (Eds.), *Models and Techniques in Computer Animation*, Tokyo: Springer-Verlag, 1993, 75–93.

[18] Lindsey, W. C.
Error probabilities for Ricean fading multichannel reception of binary and N-ary signals.
IEEE Transactions on Information Theory, **10** (Oct. 1964), 339–350.

Michael A. Jensen (S'93—M'95—SM'01) received the B.S. (summa cum laude) and M.S. degrees in electrical engineering from Brigham Young University (BYU), Provo, UT, in 1990 and 1991, respectively, and the Ph.D. in electrical engineering at the University of California, Los Angeles (UCLA) in 1994.

From 1989 to 1991 he was a graduate research assistant in the Lasers and Optics Laboratory at BYU. In 1990 he received a National Science Foundation Graduate Fellowship. From 1991 to 1994, he was a graduate student researcher in the Antenna Laboratory at UCLA. Since 1994, he has been at the Electrical and Computer Engineering Department at BYU where he is currently a professor. His main research interests include antennas and propagation, MIMO wireless communications, numerical electromagnetics, and optical fiber communications.

Dr. Jensen currently serves as a member of the Administrative Committee and the Joint Meetings Committee for the IEEE Antennas and Propagation Society and has served the society as vice-chair and technical program chair for several symposia. He was awarded the H. A. Wheeler paper award in the *IEEE Transactions on Antennas and Propagation* in 2002, and best student paper award at the 1994 IEEE International Symposium on Antennas and Propagation. He is a member of Eta Kappa Nu and Tau Beta Pi.

Michael Rice (M'82—SM'98) received a B.S.E.E. from Louisiana Tech University, Rustin, in 1987 and his Ph.D. from Georgia Tech, Atlanta, in 1991.

He was with Digital Transmission Systems, Inc. in Atlanta and joined the faculty at Brigham Young University in 1991 where he is currently the Jim Abrams Professor in the Department of Electrical & Computer Engineering. He was a NASA/ASEE Summer Faculty Fellow at the Jet Propulsion Laboratory during 1994 and 1995 where he worked on land mobile satellite systems. During the 1999–2000 academic year, he was a visiting scholar at the Communication Systems and Signal Processing Institute at San Diego State University. His research interests are in the area of digital communication theory and error control coding with a special interest in applications to telemetering and software radio design. He has been a consultant to both government and industry on telemetry related issues.

Dr. Rice is a member of the IEEE Communications Society. He was chair of the Utah Section of IEEE from 1997 to 1999 and chair of the Signal Processing & Communications Society Chapter of the Utah Section from 2002 to 2003.

Adam L. Anderson (S'00) received the B.S. (2002) and M.S. (2004) degrees in electrical engineering from Brigham Young University, Provo, UT, and is currently working toward a Ph.D. degree in electrical engineering at the University of California, San Diego.

His current research interests focus on multiple-input multiple-output (MIMO) systems in mobile ad hoc networks (MANET).